**Supplemental information inventory:**

**Supplemental Figures and Legends:**

S1 (related to Figure 1): The use of #123-Cre mice for the deletion of Gsα in immature OSNs.

S2 (related to Figures 4 and 5): OSNs expressing G-protein coupling M71 mutant ORs are gradually eliminated from the epithelium and their axons are rarely observed on the bulb.

S3 (related to Figures 6 and 8): O/E2-M71-GFP mice ubiquitously express *M71*.

S4 (related to Figures 7 and 9): O/E2-M71 expression affects axonal projections of OSNs expressing endogenous ORs.

S5 (related to all Figures): Previously described mouse strains with gene-targeted OR mutations and their abbreviations that were used throughout the study.

**Supplemental Tables:**

S1 (related to Figures 1, 5, 6, S1, and S3): List of ISH probes that were used.

S2 (related to Figures 6 and 9): List of nanostring probes that were used.

## Supplemental Figures and tables.

**Figure S1. The use of #123-Cre mice for the deletion of Gsα in immature OSNs.**

(A) Three-colour ISH on coronal sections of PD6 MOE of #123-Cre x ROSA26(R26)-STOP-tauGFP mice. Riboprobes were used against *Cre* (red-A1,-A2), *Gap43* (green-A2) and *Omp* (blue-A2). *Cre* is expressed before the onset of Gap43. (B, C) Three-colour ISH on coronal sections of PD6 MOE of #123-Cre x R26-STOP-tauGFP mice with probes against bovine *tau* (red-B1, -B2, -C1, -C2), *Gap43* (green-B2, C2) and *Omp* (blue-B2,-C2). Expression of tau is only observed after removal of the loxp flanked transcriptional stop cassette of the R26-STOP-tauGFP allele, which is therefore an indicator of successful Cre recombination. Tau is expressed before the onset of Gap43. (D, F) Three-colour ISH on coronal sections of PD6 Gs WT (D) and Gs cKO (F) MOE with probes against *Gnas* (red-D1,-D2, -F1, -F2), *Gap43* (green-D2, -F2) and *Omp* (blue-D2, -F2). In Gs cKO mice, *Gnas* expression is clearly more basal throughout the whole epithelium, indicating that it is mostly expressed in the basal progenitors. (E, G) Three-colour ISH on coronal sections of PD6 Gs WT and Gs cKO MOE with probes against *Gnal* (red), *Gap43* (green) and *Omp* (blue). (H, I) Intrinsic GFP fluorescence observed in coronal sections of the MOB from #123-Cre x R26-STOP-tauGFP (= Gs WT) in H1 and high magnification H2 and #123-Cre x R26-STOP-tauGFP x Gnas-E1$^{fl/fl}$ (= Gs cKO) mice in I1 and high magnification I2. Intrinsic GFP reporter expression is only seen after Cre recombination. DAPI counterstain. (J) The A-P position of individual M72 (PD10, Gs WT n=8, Gs cKO n=8) and MOR23 (PD21 Gs WT n=8, Gs cKO n=8) glomeruli in Gs WT and cKO animals. (K) Higher magnification of Gs WT, Figure 1A2 (see also D2 above), *Gnas* (red), *Gap43* (green), showing that some *Gap43+* cells express *Gnas* (highlighted with arrows). (L) Lower magnification of posteriorly projecting lateral M71 glomerulus in Golf KO mice (PD11, scale bar: 250μm). The M71-GFP mutation is homozygous.

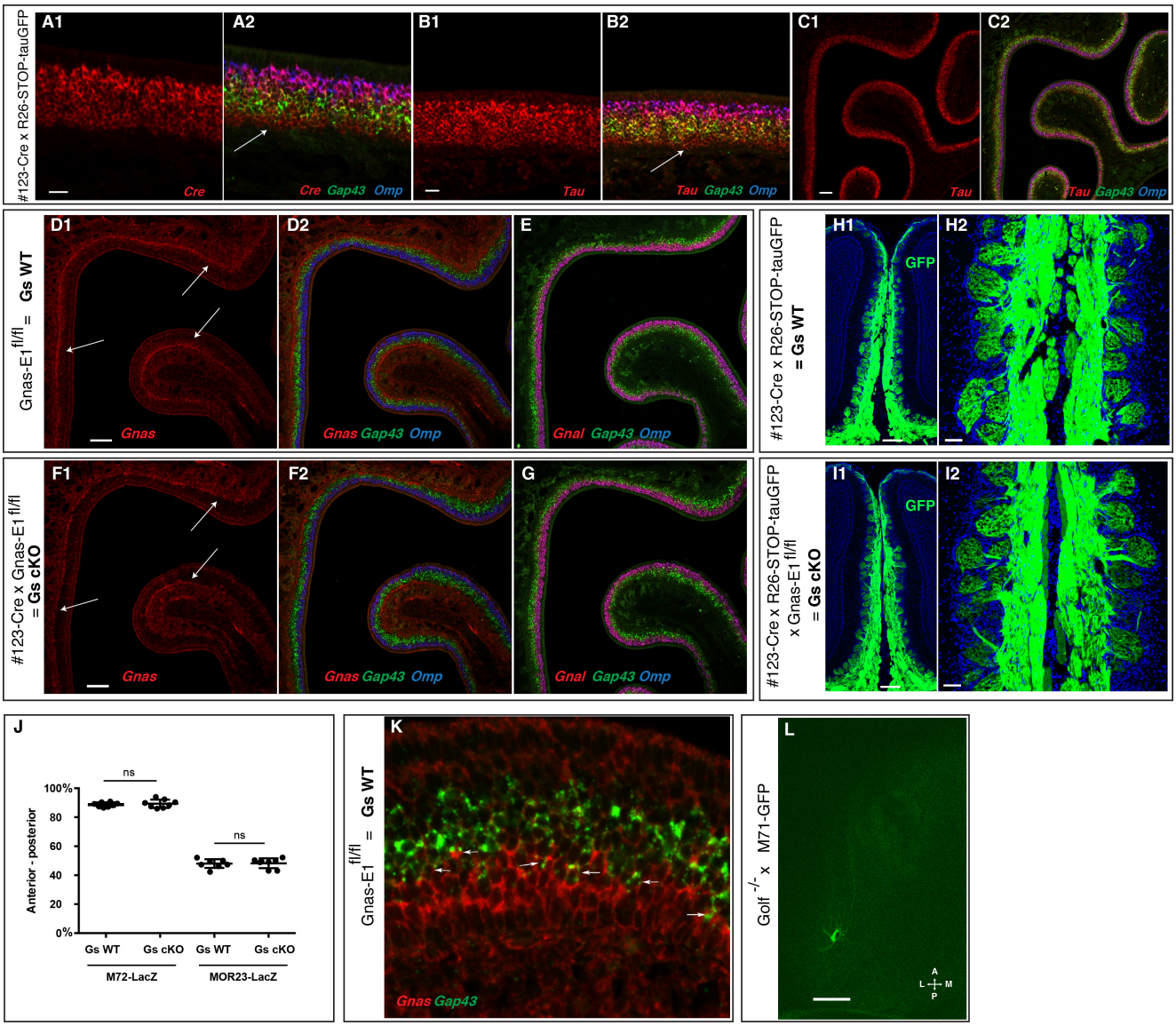
#123-Cre x R26-STOP-tauGFP
A1
Cre
A2
Cre Gap43 Omp
B1
Tau
B2
Tau Gap43 Omp
C1
Tau
C2
Tau Gap43 Omp
Gnas-E1fl/fl = Gs WT
D1
Gnas
D2
Gnas Gap43 Omp
E
Gnal Gap43 Omp
#123-Cre x R26-STOP-tauGFP = Gs WT
H1
GFP
H2
#123-Cre x Gnas-E1fl/fl = Gs cKO
F1
Gnas
F2
Gnas Gap43 Omp
G
Gnal Gap43 Omp
#123-Cre x R26-STOP-tauGFP x Gnas-E1fl/fl = Gs cKO
I1
GFP
I2
J
Anterior - posterior
100%
80
60
40
20
0%
ns
ns
Gs WT
Gs cKO
Gs WT
Gs cKO
M72-LacZ
MOR23-LacZ
K
Gnas-E1fl/fl = Gs WT
Gnas Gap43
L
Golf -/- x M71-GFP
A
L
M
P

**Figure S2. OSNs expressing G-protein coupling M71 mutant ORs are gradually eliminated from the epithelium and their axons are rarely observed on the bulb.**

Medial view of X-gal-stained wholemounts of (A) M71-LacZ (3wo) and (B) M71(RDY)-lacZ (PD10) mice. (C) Higher-magnification of X-gal-stained M71(RDY) MOE (PD10), shows that OSNs poorly project axons, which appear short and stunted. (D) Number of X-gal+ OSNs on wholemounts of M71(RDY)-LacZ turbinates at indicated postnatal days (mean ± SEM, n=6-11 for each time point). (E) IHC was performed against: β-galactosidase for counting M71 and M71(RDY) OSNs; GFP for counting M71(RDY)-caGs OSNs; and DsRed for counting MOR23(RDY)→M71-caGs OSNs on coronal sections at PD21. Every 10th section was collected from anterior to posterior and 49 sections were counted per mouse. Data are mean ± SEM (n=3). One-way ANOVA and Newman–Keuls post test (D, E). *$p < 0.05$, **$p < 0.01$, ***$p < 0.001$. Scale bars, 500 μm.

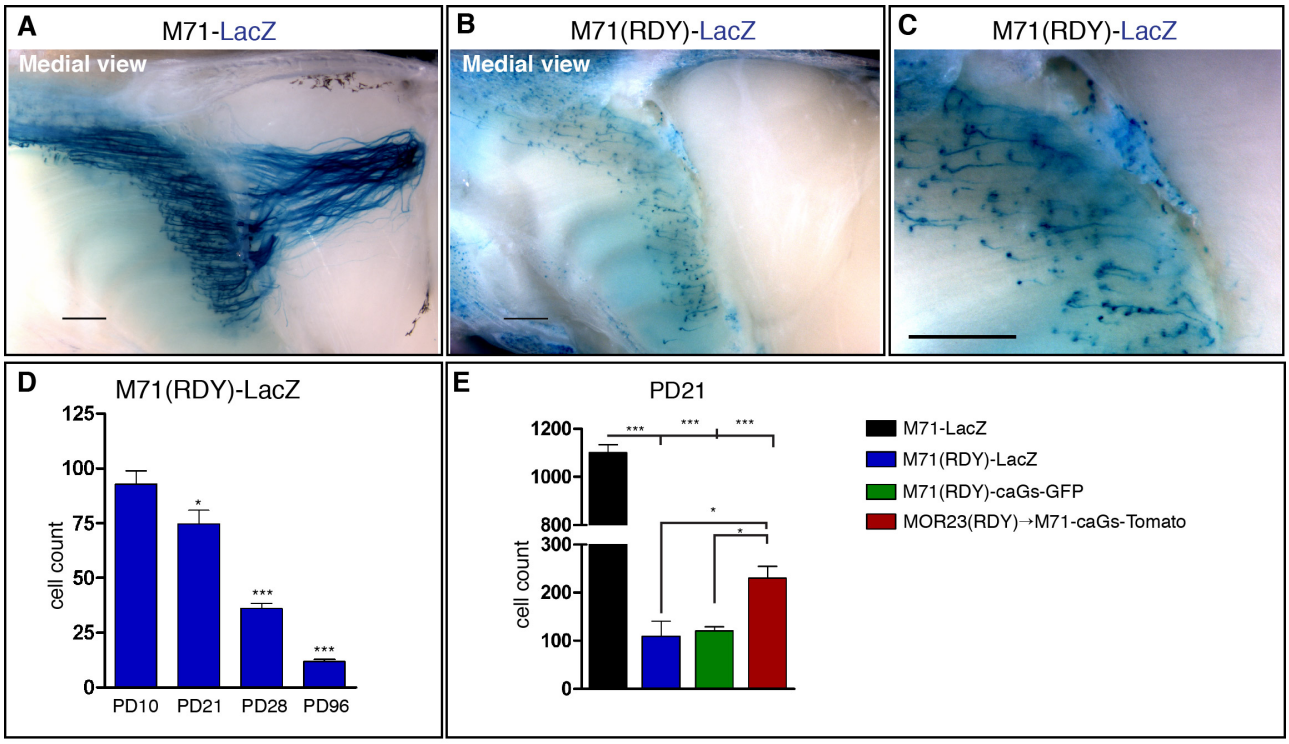

**Figure S3. O/E2-M71-GFP mice ubiquitously express *M71*.**

(A) Two-colour ISH on coronal sections of the MOE from WT mice with probes against *M71* (red-A1) plus *O/E2* (green-A2). (B) Three-colour ISH against *Gap43* (green), *Omp* (blue) and the sustentacular marker *Cbr2* (red), in the MOE of WT mice. (C) Two-colour ISH on coronal sections of the MOE from heterozygous O/E2-M71-GFP mice with probes against *M71* (red-C1) plus *O/E2* (green-C2). Some red labelled neurons in the dorsal epithelium appeared more intense suggesting that endogenous M71/M72 ORs are expressed at a slightly higher level than those from the O/E2 promoter. (D) Three-colour ISH against *Gap43* (green), *Omp* (blue) and the sustentacular marker *Cbr2* (red), in the MOE of heterozygous O/E2-M71-GFP mice. Scale bars, 100 μm (A2, C2), 50 μm (B,D).

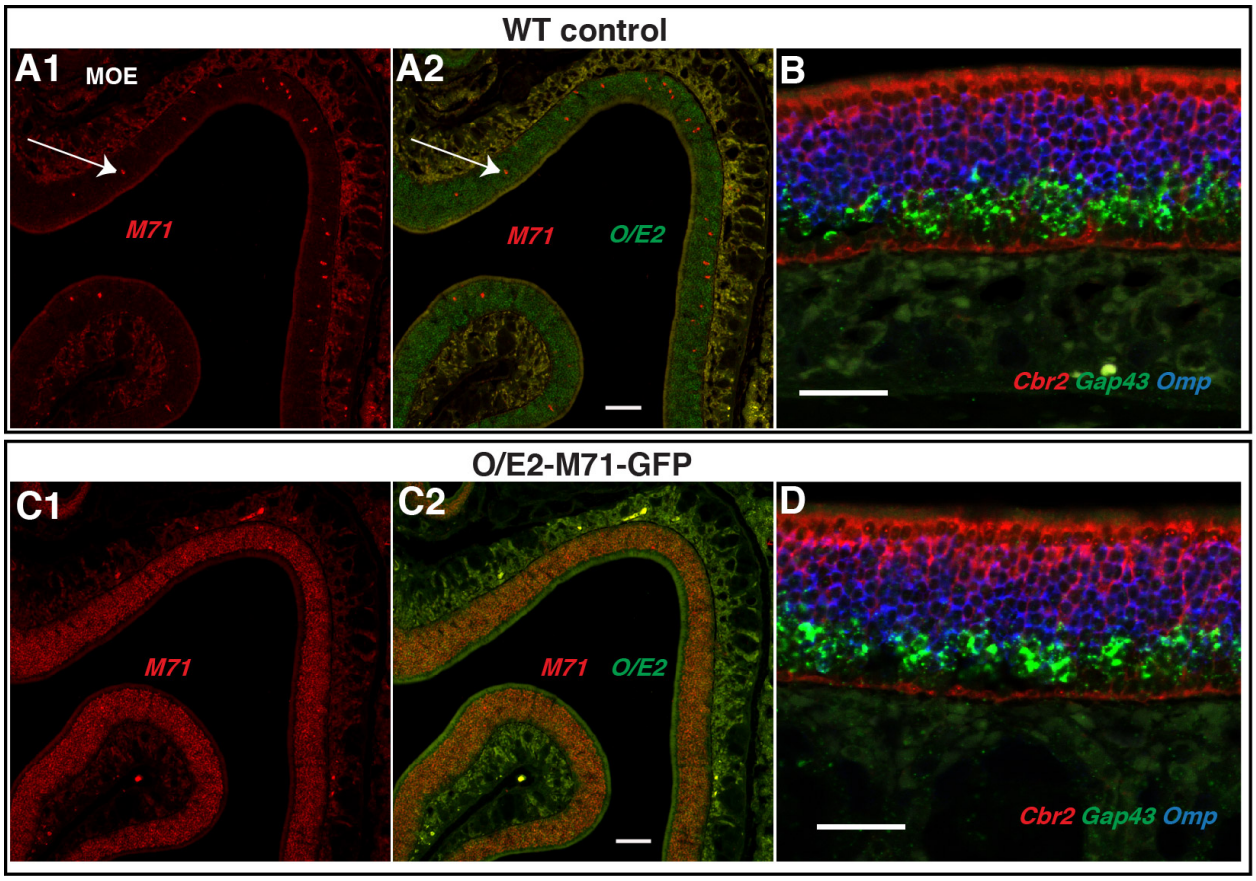

**Figure S4. O/E2-M71 expression affects axonal projections of OSNs expressing endogenous ORs.**

(A) In the P-LacZ transgenic mice, wholemount X-gal staining of the dorsal bulb labels axons expressing class II ORs, while the unlabelled butterfly-shaped pattern corresponds to the class I and TAAR domains [48]. Interestingly, in O/E2-M71-GFP mutants (right, O/E2 +/-), this butterfly pattern was disrupted, as LacZ+ axons now traversed through the dorsal-medial regions. (B-C) Wholemount X-gal staining of (B) MOR23-lacZ and (C) M71-lacZ OSNs in O/E2-M71-GFP heterozygous mice. Three representative examples are shown for two ORs, showing how O/E2-M71 expression alters the axonal projections of OSNs. Scale bars, 500 μm.

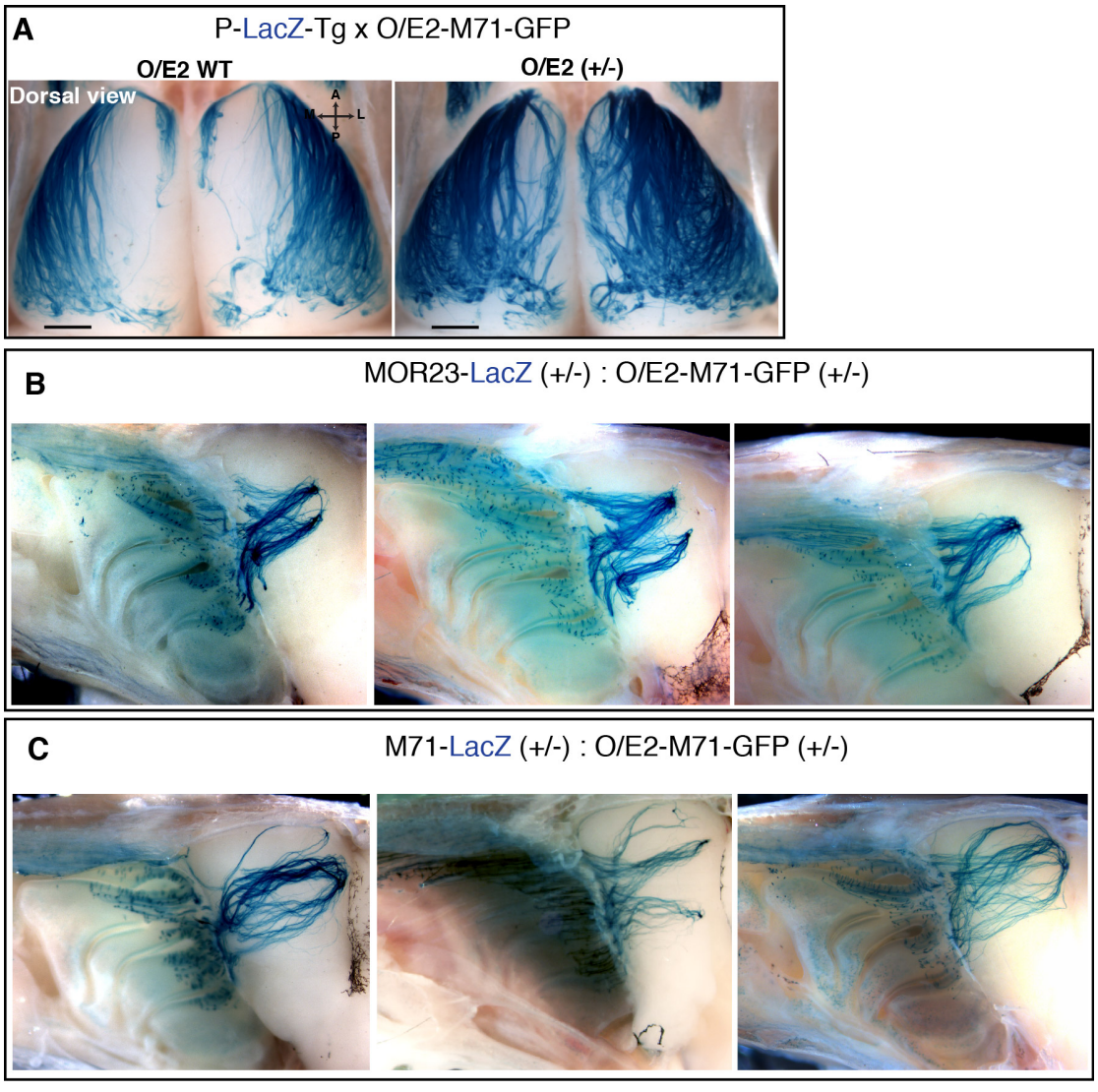

**Figure S5. Previously described mouse strains with gene-targeted OR mutations and their abbreviations that were used throughout the study.**

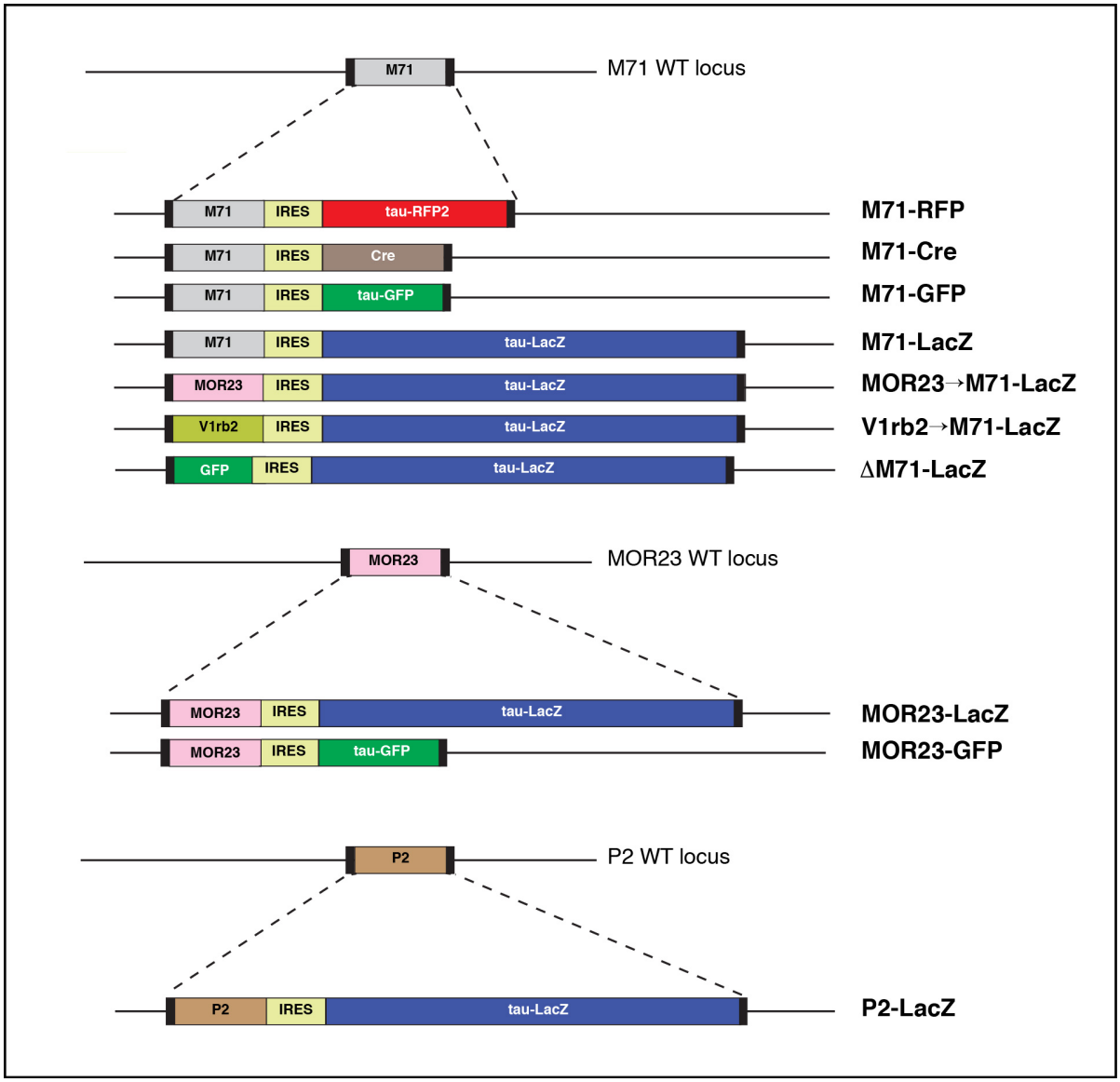

**Table S1. List of ISH Probes that were used.**

| Riboprobe | Sequence | Reference |
|---|---|---|
| *Gnas* | nt 408–1512 from NM_001077510.2 | (Omura et al., 2014) |
| *Gnal* | nt 1–1106 from NM_ 010307 | (Omura et al., 2014) |
| *Omp* | nt 820-2891 from U01213 | (Ishii et al., 2004) |
| *Gap43* | nt 147-860 from NM_008083 | (Ishii et al., 2004) |
| *Cbr2* | nt 5-466 from BC010758 | (Ishii et al., 2004) |
| *Adcy3* | nt 2853-3559 from NM_001159536 | (Hirota et al., 2007) |
| *Cre* | nt 485-1516 from X03453 | (Li et al., 2004) |
| *mCherry (for tdTomato)* | nt 21-512 from AY678264 | (Omura et al., 2014) |
| *GFP* | nt 97-816 from U76561.1 | (Li et al., 2004) |
| *tau (*bovine) | nt 102-621 from NM_174106.2 | (Ishii and Mombaerts, 2008) |
| *lacZ* | nt 73035-73522 from U73857.1 | |
| *O/E2* | nt 2353-3392 from NM_001113415.1 | |
| *M71* | nt 144-1013 from NM_207664.2 | (Fuss et al., 2007) |
| *Olfr3 (class II mix)* | nt 17-871 from NM_206903.1 | (Omura et al., 2014) |
| *Olfr62 (class II mix)* | nt 167-883 from NM_146315.2 | (Omura et al., 2014) |
| *Olfr54 (class II mix)* | nt 1-942 from NM_010997.1 | (Omura et al., 2014) |
| *Olfr749 (class II mix)* | nt 73-984 from NM_020288.2 | (Fuss et al., 2007) |

**Table S2. List of NanoString probes that were used.**

| Gene | Accession number | Target region |
|---|---|---|
| *Omp* (ref gene 1) | NM_011010.2 | 1148-1247 |
| *Gnal* (ref gene 2) | NM_177137.4 | 3129-3228 |
| *Adcy3* (ref gene 3) | NM_001159537.1 | 3377-3476 |
| *Ano2* (ref gene 4) | NM_153589.2 | 3346-3445 |
| *Cnga2* (ref gene 5) | NM_007724.2 | 54-153 |
| *Olfr1015* | NM_146571.2 | 761-860 |
| *Olfr1156* | NM_146817.2 | 397-496 |
| *Olfr124* | NM_147062.2 | 536-635 |
| *Olfr1301* | NM_146887.1 | 351-450 |
| *Olfr15* | NM_008762.2 | 31-130 |
| *Olfr1507* | NM_001170918.1 | 731-830 |
| *Olfr1508* | NM_020513.2 | 783-882 |
| *Olfr1509* | NM_020514.2 | 371-470 |
| *Olfr1511* | NM_146271.2 | 196-295 |
| *Olfr16* | NM_008763.2 | 401-500 |
| *Olfr160* | NM_030553.2 | 385-484 |
| *Olfr166* | NM_147068.1 | 39-138 |
| *Olfr17* | NM_020598.1 | 754-853 |
| *Olfr2* | NM_010983.1 | 771-870 |
| *Olfr309* | NM_001011866.1 | 401-500 |
| *Olfr6* | NM_206897.1 | 767-866 |
| *Olfr713* | NM_147034.1 | 837-936 |
| *Olfr73* | NM_054090.1 | 406-505 |
| *Olfr78* | NM_001168503.1 | 661-760 |
| *Kirrel2* | NM_172898.3 | 2763-2862 |
| *Kirrel3* | NM_001190914.1 | 113-212 |
| *Epha5* | NM_007937.3 | 2006-2105 |
| *Efna5* | NM_207654.2 | 1131-1230 |
| *Sema3f* | NM_011349.3 | 2576-2675 |

| | | |
|---|---|---|
| *Sema3a* | NM_009152.3 | 3116-3215 |
| *Nrp2* | NM_001077403.1 | 611-710 |
| *Nrp1* | NM_008737.2 | 3596-3695 |
| *Plxna1* | NM_008881.2 | 8201-8300 |
| *Plxna3* | NM_008883.2 | 6153-6252 |